

1

What Instrumental Approaches are Available

The fantastic development of mass spectrometry (MS) in the last 30 years has led this technique to be applied practically in all analytical fields. We focus our attention on the application in the organic, biological and medical fields which nowadays represent the environment in which MS finds the widest application. This chapter is devoted to a short description of the different instrumental approaches currently in use and commercially available.

MS is based on the production of ions from the analyte, their analysis with respect to their mass to charge ratio (m/z) values and their detection. Consequently, at instrumental level three components are essential to perform mass spectrometric experiment: (i) ion source; (ii) mass analyser; and (iii) detector (Figure 1.1). Of course, the performances of these three components reflect on the quality of both quantitative and qualitative data. It must be emphasized that generally these three components are spatially separated (Figure 1.1a) and only in two cases [Paul ion trap and Fourier transform mass spectrometer without external source(s)] can they occupy the same physical space and, consequently, the ionization and mass analysis must be separated in time (Figure 1.1b).

1.1 ION SOURCES

The ion production is the phenomenon which highly affects the quality of the mass spectrometric data obtained. The choice of the ionization

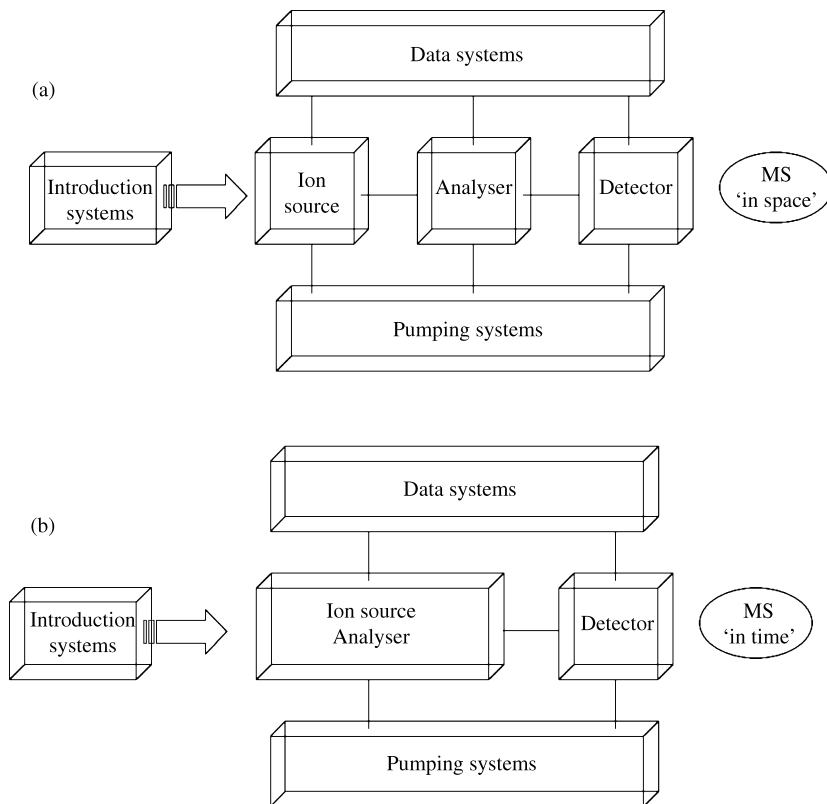


Figure 1.1 Schemes of MS systems 'in space' (a) and 'in time' (b)

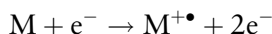
method to be employed is addressed by the physico-chemical properties of the analyte(s) of interest (volatility, molecular weight, thermolability, complexity of the matrix in which the analyte is contained).

Actually the ion sources usually employed can be subdivided into two main classes: those requiring sample in the gas phase prior to ionization; and those able to manage low volatility and high molecular weight samples.

The first class includes electron ionization (EI) and chemical ionization (CI) sources which represent those worldwide most diffused, due to their extensive use in GC/MS systems. The other ones can be further divided into those operating with sample solutions [electrospray ionization (ESI), atmospheric pressure chemical ionization (APCI), atmospheric pressure photoionization (APPI)] and those based on the contemporary sample desorption and ionization from a solid substrate [matrix - assisted laser desorption/ionization (MALDI) and LDI].

1.1.1 Electron Ionization

EI is based on the interaction of an energetic (70 eV) electron beam with the sample vapour (at a pressure in the range 10^{-7} – 10^{-5} Torr) (Figure 1.2). This interaction leads to the production of a series of ions related to the chemical properties of the compound(s) under study. The theoretical treatment of EI is beyond the scope of the present book and it is possible to find it in many publications.¹ For the present discussion it is enough to consider that EI generally leads to a molecular ion $M^{+\bullet}$, originating by the loss of an electron from the neutral molecule:



and to a series of fragments, generally highly diagnostic from the structural point of view:

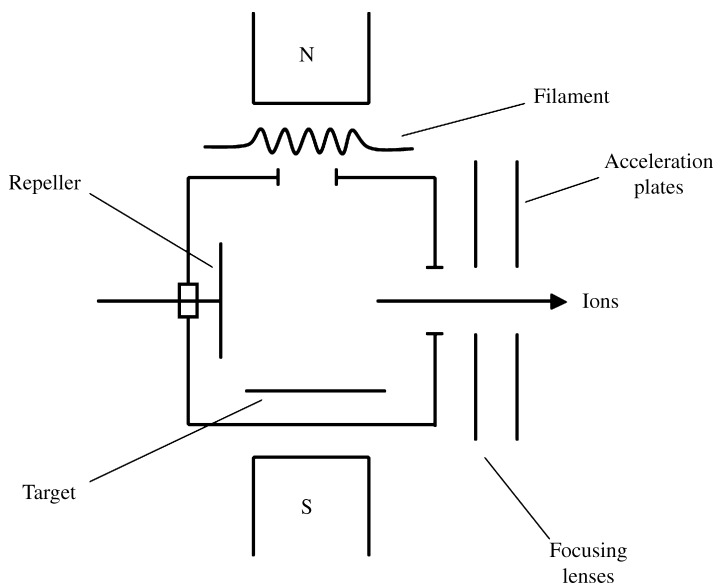
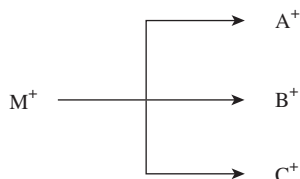


Figure 1.2 Scheme of an electron ionization (EI) ion source. The electrons are generated by the filament, accelerated by the potential between the filament and ion chamber, and focused on the target. A permanent magnet (N–S) is mounted axially to the electron beam to induce a cycloidal pathway (and a consequent increase of electron-neutral interactions), leading to higher ion production yield. The repeller electrode favours the acceleration field penetration, leading to higher ion extraction



Some of them originate from simple bond cleavages, while some others are produced through rearrangement processes. What must be emphasized is that EI leads to well reproducible mass spectra. In other words, by different EI sources spectra practically superimposable are obtained and this is the reason for which the only spectrum libraries available are those based on EI data.

The main efforts done in the last decade in the EI field are due to the development of ion sources with the highest possible ion yield. To reach this aim, on the one hand an optimization of ion source geometry has been performed (this has been achieved by the development of suitable ion optics to increase either the ion production or the ion extraction), on the other, to make inert the ion source walls (originally in stainless steel) so as to avoid the sample loss due to its pyrolysis on the hot metallic surface.

The quantitative data obtained by EI can be strongly affected mainly by two parameters: the first related to sample loss (due to problems related to sample injection lines and to 'open' source configuration as well as to thermal decompositions occurring in injection lines and/or source), while the second can be related to a decreased efficiency of ion extraction (nonoptimized extraction field, field modification due to the presence of polluted surfaces). These two aspects reflect not only on the limit of detection (LOD) of the system but also on the linearity of the quantitative response.

The ion most diagnostic from the qualitative point of view is usually considered the molecular one ($M^{+\bullet}$). However, wide classes of compounds, easily vaporized, do not lead to the production of $M^{+\bullet}$. This is due to the energetics of EI induced decomposition processes. In other words if a decomposition process is energetically favoured (with a particularly low critical energy) it takes place immediately, due to the internal energy content of $M^{+\bullet}$. To overcome this problem in the 1960s a new ionization method was developed, based on gas-phase chemical reactions.

1.1.2 Chemical Ionization

To obtain a lower energy deposition in the molecule of interest, reflecting in the privileged formation of charged molecular species, in the 1960s CI

methods were proposed.² They are based on the production in the gas phase of acidic or basic species, which further react with a neutral molecule of analyte leading to $[M + H]^+$ or $[M - H]^-$ ions, respectively. Generally, protonation reactions of the analyte are those more widely employed; the occurrence of such reactions is related to the proton affinity (PA) of M and the reactant gas, and the internal energy of the obtained species are related to the difference between these proton affinities. Thus, as an example, considering an experiment performed on an organic molecule with PA value of 180 kcal/mol (PA_M), it can be protonated by reaction with CH_5^+ ($PA_{CH_4} = 127$ kcal/mol), H_3O^+ ($PA_{H_2O} = 165$ kcal/mol), but not with NH_4^+ ($PA_{NH_3} = 205$ kcal/mol).³ This example shows an important point about CI: it can be effectively employed to select species of interest in complex matrices. In other words, by a suitable selection of a reacting ion $[AH]^+$ one could produce $[MH]^+$ species of molecules with PA higher than that of A. Furthermore the extension of fragmentation can be modified in terms of the difference of $[PA_M - PA_A]$.

From the operative point of view CI is simply obtained by introducing the neutral reactant species inside an EI ion source in a 'close' configuration, by which quite high reactant pressure can be obtained (Figure 1.3).

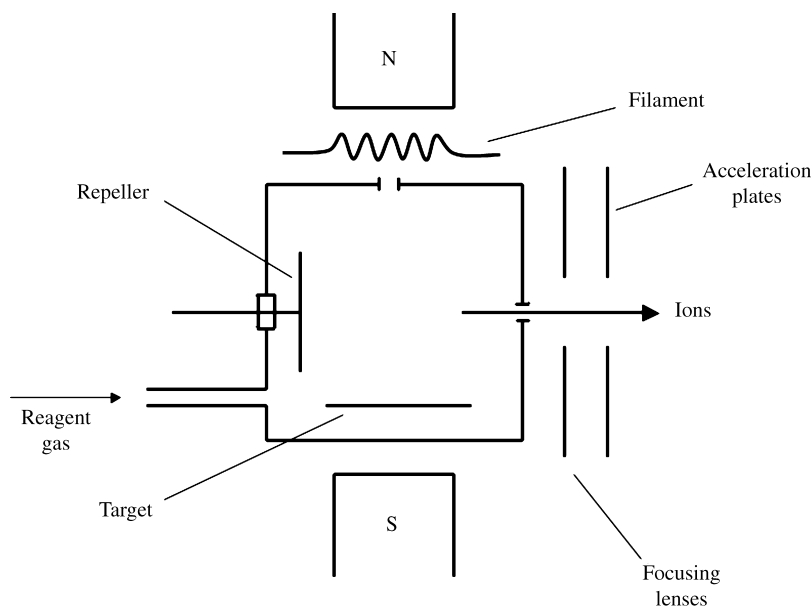


Figure 1.3 Scheme of a chemical ionization (CI) ion source. The electron entrance and ion exit holes are of reduced dimension in order to obtain, inside the ion chamber, effective pressure of the reagent gas

If the operative conditions are properly set the formation of abundant $[AH]^+$ species (or, in the case of negative ions B^-) is observed in high yield. Of course, attention must be paid in particular in the case of quantitative analysis to reproduce carefully these experimental conditions, because they reflect substantially on the LOD values.

CI, as well as EI, requires the presence of samples in vapour phase and consequently it cannot be applied for nonvolatile analytes. Efforts have been made from the 1960s to develop ionization methods overcoming these aspects and, among them, field desorption (FD)⁴ and fast atom bombardment (FAB)⁵ resulted in highly effective methods and opened new applications for mass spectrometry. More recently new techniques have become available and are currently employed for nonvolatile samples: APCI,⁶ ESI,⁷ APPI⁸ and MALDI⁹ represent nowadays the most used for the analysis of high molecular weight, high polarity samples.

For these reasons, we describe these methods.

1.1.3 Atmospheric Pressure Chemical Ionization

APCI⁶ was developed starting from the consideration that the yield of a gas-phase reaction does not depend only on the partial pressure of the two reactants, but also on the total pressure of the reaction environment. For this reason the passage from the operative pressure of 0.1–1 Torr, present inside a classical CI source, to atmospheric pressure would, in principle, lead to a relevant increase in ion production and, consequently, to a relevant sensitivity increase.

At the beginning of the research devoted to the development of the APCI method, the problem was the choice of the ionizing device. The most suitable and effective one was, and still is, a corona discharge. The important role of this ionization method mainly lies in its possible application to the analysis of compounds of interest dissolved in suitable solvents: the solution is injected in a heated capillary (typical temperatures in the range 350–400 °C), which behaves as a vaporizer. The solution is vaporized and reaches outside from the capillary the atmospheric pressure region where the corona discharge takes place. Usually the vaporization is assisted by a nitrogen flow coaxial to the capillary (Figure 1.4). The ionization mechanism is typically the same present in CI experiments (Figure 1.5). The solvent molecules, present in high abundance, are statistically privileged to interact with the electron beam originated from the corona discharge; the ions so formed react with other solvent molecules leading to

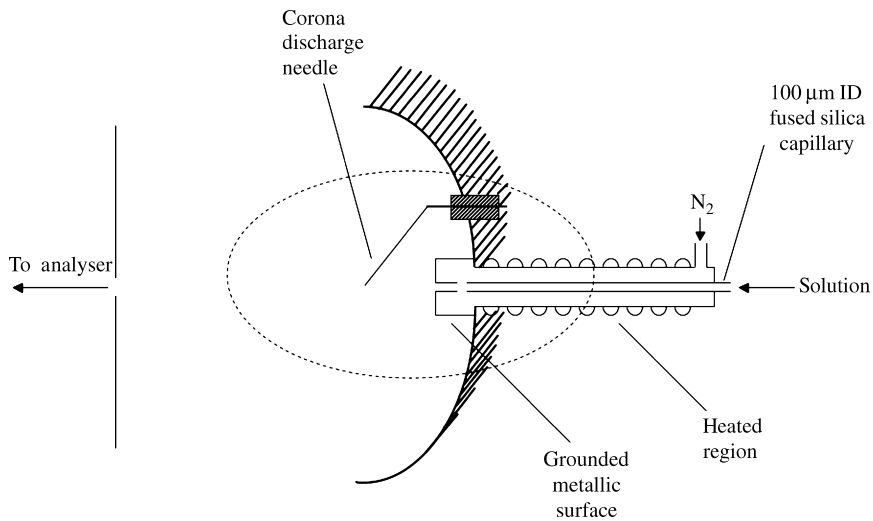


Figure 1.4 Scheme of an APCI ion source

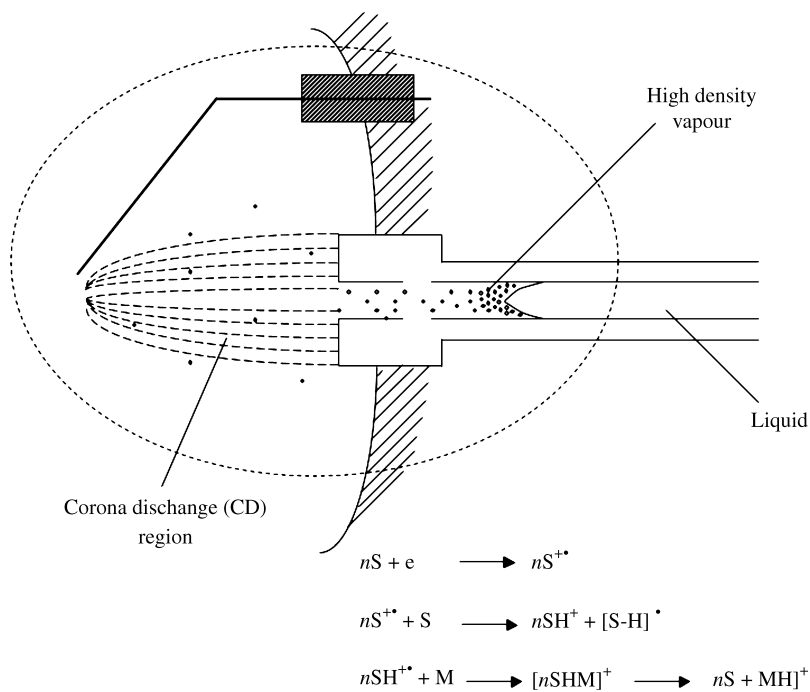


Figure 1.5 Corona discharge region of an APCI source and reactions occurring in it

protonated (in the case of positive ions analysis) or deprotonated (negative ions analysis) species, which are the reactant for the analyte ionization. One problem which, at the beginning of its development, APCI exhibited was the presence of analyte molecules still solvated, i.e. the presence of clusters of analyte molecules with different numbers of solvent molecules. To obtain a declustering of these species, different approaches have been proposed, among which nonreactive collision with target gases (usually nitrogen) and thermal treatments are those considered most effective and currently employed. Different instrumental configurations, based on a different angle between the vaporizer and entrance capillary (or skimmer) have been proposed; 180° (in line) and 90° (orthogonal) geometries are those most widely employed.

In particular, in the case of quantitative analysis, a particular care must be devoted to finding the best operating conditions (vaporizing temperature and solution flow) of the APCI source, which lead to the most stable signals, and carefully maintaining these conditions for all the measurements.

1.1.4 Electrospray Ionization

ESI⁷ is obtained by injection, through a metal capillary line, of solutions of analyte in the presence of a strong electrical field. The production of ions by ESI can be considered as due to three main steps: (i) production of charged drops in the region close to the metal capillary exit; (ii) fast decreasing of the charged drop dimensions due to solvent evaporation and, through phenomena of coulombic repulsion, formation of charged drop of reduced dimension; (iii) production of ions in the gas phase originated from small charged droplets.

The experimental device for an ESI experiment is shown in Figure 1.6. The analyte solution exits from the metal capillary (external diameter, r_c , in the order of 10^{-4} m) to which a potential (V_c) of 2–5 kV is applied; the counter electrode is placed at a distance (d) ranging from 1 to 3 cm. This counter electrode in an ESI source is usually a skimmer with a 10 μ orifice or an ‘entrance heated capillary’ (internal diameter 100–500 μ ; length 5–10 cm), which represents the interface to the mass spectrometric analyser. Considering the thickness of the metal capillary, the electrical field (E_c) close to it is particularly high. For example, for $V_c=2000$ V, $r_c=10^{-4}$ m and $d=0.02$ m, an E_c in the order of 6×10^6 V/cm has been calculated by Pfeifer and Hendricks.¹⁰ This

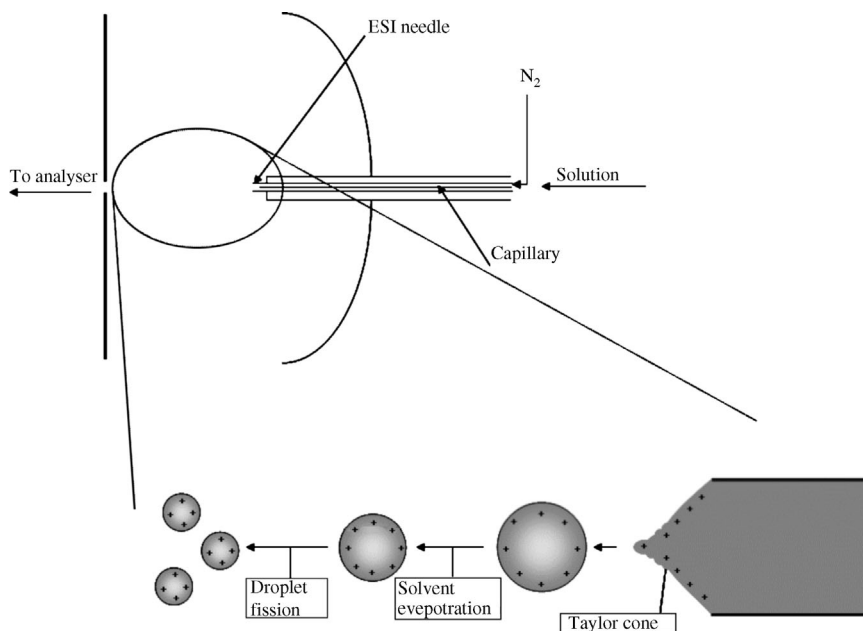


Figure 1.6 Scheme of ESI ion source and enlarged view of droplet generation region. (Taylor cone and droplet dimension are not to the same scale)

electrical field interacts with solution and the charged species present inside the solution move in the field direction, leading to the formation of the so called ‘Taylor cone’.¹¹ If the electrical field is high enough, a spray is formed from the cone apex, consisting of small charged droplets. In the case of positive ion analysis, i.e. when the needle is placed at a positive voltage, the droplets bear positive charge and vice versa in the case of negative ion analysis. A charged drop moves through the atmosphere for the field action in the direction of the counter electrode. The solvent evaporation leads to the reduction of the drop dimensions and to a consequent increase of the electrical field perpendicular to the droplet surface. For a specific value of droplet radius the ion repulsion becomes stronger than surface tension and in these conditions the droplet explosion takes place.

Two mechanisms have been proposed for the formation of gaseous ions from small charged droplets. The first model, called ‘charge residue mechanism’ (CRM) was proposed by Dole in 1968¹² and describes the process as sequential scissions leading to the production of small droplets bearing one or more charges but only one analyte molecule. When the last, few solvent molecules evaporate the charge(s) remains

deposited on the analyte structure, which gives rise to the most stable gaseous ion.

More recently, Iribarne and Thomson have proposed a different mechanism, describing the direct emission of gaseous ions from the droplets, after it has reached a certain dimension.¹³ This process, called the 'ion evaporation mechanism' (IEM) is predominant on the coulombic fission for droplets of radius, r , lower than $10\ \mu$.

From the above, the reader can consider the factors which can affect the ion production and consequently the sensitivity and reproducibility in ESI measurements. The ion intensity exhibits with respect to analyte concentration a typical trend, analogous to that reported, as an example, in Figure 1.7. A linear portion with a slope of about 1 is present for low concentration until 10^{-6} M, followed by a slow saturation with a weak intensity decreasing at the highest concentrations (10^{-3} M). The linear portion, where intensity is proportional to concentration, is the only region suitable for quantitative analysis. The general trend of the plot can be explained considering that in the system there is not just a single analyte: further electrolytes are always present, for example, impurities, co-analytes and buffer. It should be emphasized that for analyte concentrations lower than 10^{-5} M, the electrospray phenomenon occur due to the presence of electrolytes as impurities, which lead to the electrical conductivity necessary for the 'Taylor cone' production.

Also, in the case of ESI sources, 'in line' or 'orthogonal' geometries have been proposed and employed.

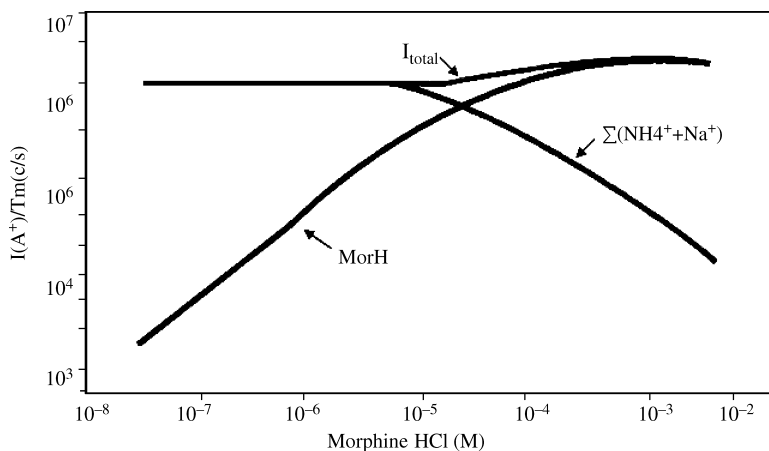


Figure 1.7 Plot of ion intensity *vs* analyte (morphine HCl) concentration obtained by ESI experiments. Reprinted from P. Kébarle and L. Tang, *Anal. Chem.* 65, 980A (1993), with permission from the American Chemical Society

1.1.5 Atmospheric Pressure Photoionization

A method recently developed consists in the irradiation, by a normal krypton (Kr) lamp, of the vaporized solution of the sample of interest at atmospheric pressure (APPI).⁸ The instrumental set up is very similar to that already described for the APCI system (Figure 1.8). In this case, the needle for corona discharge is no longer present, while the solution vaporizer is exactly the same as for the APCI source. On a side of the source the Kr lamp is mounted, so that the vapour solution can be irradiated by photons with energies up to 10.6 eV. The photoionization follows a simple general rule: a molecule with ionization energy (IE_M) can be ionized by photons with energy $E_\nu = h\nu$ only when:

$$IE_M \leq E_\nu$$

Considering that the most of solvents employed in liquid chromatography (LC) methods have an IE higher than 10.6 eV and consequently cannot be ionized by interaction with photon coming from the Kr lamp, the APPI method seems to be, in principle, highly effective for liquid chromatography/mass spectrometry (LC/MS) analysis of compounds

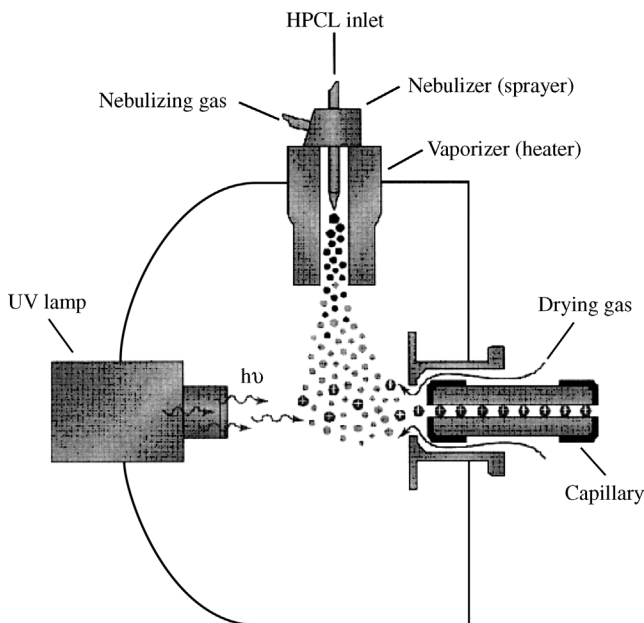


Figure 1.8 Scheme of an APPI ion source

exhibiting IE lower than 10.6 eV. In the case of compounds of interest with IE > 10.6 eV, the use of dopants (i.e. substances photoionizable acting as intermediates in the ionization of the molecule of interest) has been proposed.⁸

Some investigations have shown that some unexpected reactions can take place in the APPI source, indicating that it can be applied not only for analytical purposes but also for fundamental studies of organic and environmental chemistry.¹⁴

1.1.6 Matrix-assisted Laser Desorption/Ionisation

MALDI⁹ consists of the interaction of a laser beam with a solid sample constituted by a suitable matrix in which the analyte is present at very low molar ratio (1:10 000) (Figure 1.9). This interaction leads to the

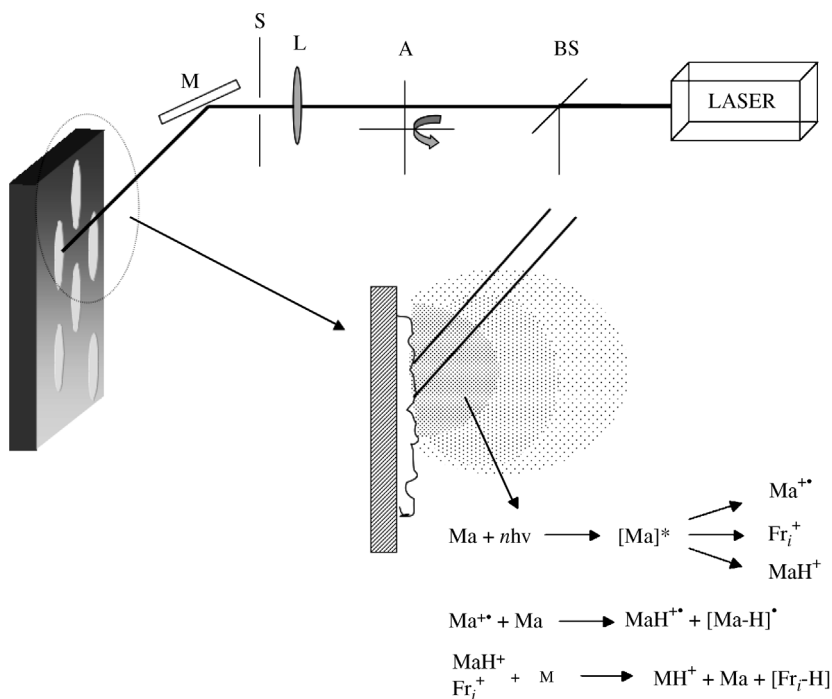


Figure 1.9 Scheme of MALDI ion source and reactions occurring in the high density plume originated by laser irradiation. BS, beam splitter (a portion of the laser beam is used to start the spectrum acquisition); A, attenuator (to regulate the laser beam intensity); L, focusing lens, S, slit; M, mirror

vaporization of a small volume of the solid sample: in the plume of the high density vapour so generated, reactive species originating for the matrix irradiation react with the neutral molecules of analyte, mainly through protonation/deprotonation mechanisms.

A detailed description of the MALDI mechanism is highly complex, due to the presence of many different phenomena:

- (i) First of all the choice of the matrix is relevant to obtain effective and well reproducible data.
- (ii) The solid sample preparation is usually achieved by the deposition on a metallic surface of the solution of matrix and analyte with concentration suitable to obtain the desired analyte/matrix ratio. The solution is left to dry under different conditions (simply at atmospheric pressure, reduced pressure or under nitrogen stream); in all cases what is observed is the formation of an inhomogeneous solid sample, due to the different crystallization rate of the matrix and analyte. Consequently, the 1:10 000 ratio is only a theoretical datum: in the solid sample different ratios will be found in different positions and the only way to overcome this is to average a high number of spectra corresponding to laser irradiation of different points.
- (iii) The photon–phonon transformation, obtained when a photon interacts with a crystal and giving information on the vibrational levels of the crystal lattice, cannot be applied in the laser induced vaporization observed in MALDI experiments, due to the inhomogeneity of the solid sample.
- (iv) The laser irradiance is an important parameter: different irradiance values lead to vapour cloud of different density and consequently different ion–molecule reactions can take place.

In other words the MALDI data originate from a series of physical phenomena and chemical interactions originating by the parameterization (matrix nature, analyte nature, matrix/analyte molar ratio, laser irradiation value, averaging of different single spectra), which must be kept under control as much as possible. However, the results obtained by MALDI are of high interest, due to its applicability in fields not covered by other ionization methods. Due to the pulsed nature of ionization phenomena (an N_2 laser operating with pulses of 10^2 ns and with a repetition rate of 5 MHz) the analyser usually employed to obtain the MALDI spectrum is the time-of-flight (TOF) one, which will be described in Section 1.2.4.

1.2 MASS ANALYSERS

The mass analysis of ions in the gas phase is based on their interaction with electrical and magnetic fields. Originally the main component of these devices was a magnetic sector which separates the ions with respect to their m/z ratio. Until the 1960s most of the mass spectrometers devoted to physics, organic and organometallic chemistry were based on this approach, and high resolution conditions were (and still are) generally acquired by the use of an electrostatic sector. The double-focusing instruments were (and are) of large dimension (at least 2 m^2) and required the use of heavy magnet and large pumping systems.

In the 1960s, mainly due to the efforts of the Paul group at Bonn University, the development of devices based on electrodynamic fields for mass analysis led to the production of quadrupole mass filters and ion traps of small dimension, so that the mass spectrometer became a bench-top instrument.

The ease of use of these devices, the ease of interfacing them with data systems and, over all, the relatively low cost were the factors that moved mass spectrometry from high level, academic environments to application laboratories, in which the instrument is considered just in terms of its analytical performances.

In this section, the analysers currently most widely employed will be described, in terms of the physical phenomena on which they are based, of their performances and their ease of use.

1.2.1 Mass Resolution

The main characteristic of a mass analyser is its resolution, defined as its capability to separate two neighbouring ions. The resolution necessary to separate two ions of mass M and $(M + \Delta M)$ is defined as:

$$R = M/\Delta M$$

Then, as an example, the resolution necessary to separate N_2^+ (exact mass = 28.006158) from CO^+ (exact mass = 27.994915) is:

$$R = M/\Delta M = 28/0.011241 = 2490$$

From the theoretical point of view, the resolution parameters can be described by Figure 1.10. It follows that a relevant parameter is the

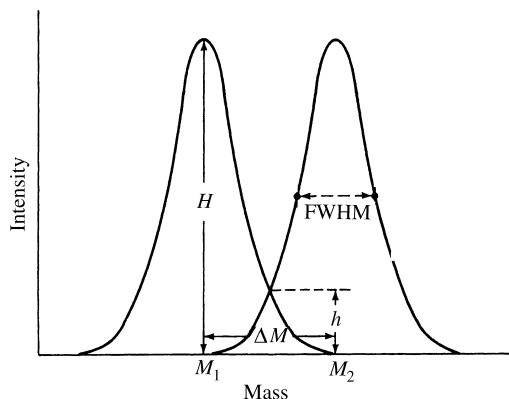


Figure 1.10 Mass resolution parameters

valley existing between the two peaks. Usually resolution data are related to 10 % valley definition.

If the peak shape is approximately gaussian the resolution can be obtained by a single peak. In fact, as shown by Figure 1.10, the mass difference, ΔM , is equal to the peak width at 5 % of its height and, accordingly to the gaussian definition, it is about two times the full width at half maximum height (FWHM). Consequently, by this approach it is possible to estimate the resolution of a mass analyser simply by looking at a single peak, without introduction of two isobaric species of different accurate mass.

The resolution present in different mass analysers can be affected by different parameters and different definitions can be employed. Thus, in the case of a magnetic sector instrument the above 10 % valley definition is usually employed, while in the case of a quadrupole mass filter the operating conditions are such to keep ΔM constant through the entire mass range. Consequently, in the case of a quadrupole mass filter the resolution will be 1000 at m/z 1000 and 100 at m/z 100, while in the case of magnetic sector the resolution will be, for example, 1000 at m/z 1000 and 10 000 at m/z 100.

This parameter will be useful to evaluate and compare the performances of different instrumental approaches.

1.2.2 Sector Analysers

At the beginning of the last century, after fundamental studies by Thompson and Aston, which led to the development of the first effective

mass spectrograph, the first sector instrument was developed by Dempster.¹⁵ As shown in Figure 1.11, in the Dempster instrument the ions are accelerated by means of a negative potential which could be changed from 500 to 1750 V. The ion beam collimated by the slit S_1 enters in uniform magnetic field B .

From the equations:

$$mv^2/2 = zV(\text{kinetic energy} = \text{potential energy}) \quad (1.1)$$

and

$$mv^2/R = zvB(\text{centrifugal force} = \text{centripetal force}) \quad (1.2)$$

it follows that:

$$m/z = B^2R^2/2V \quad (1.3)$$

where m is ion mass, z is ion charge, V is acceleration potential, v is speed acquired by the ion after acceleration and R is the circular pathway radius of the ion inside the magnetic field.

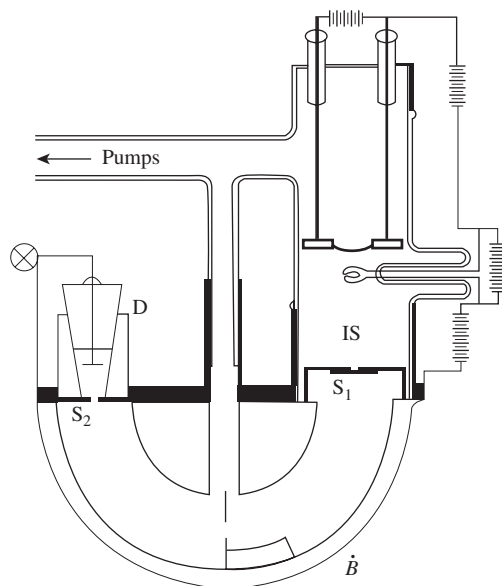


Figure 1.11 Dempster mass spectrometer. IS, ion source; S_1 , ion source slit; B , 180° magnetic field; S_2 , collector slit; D, electrostatic detector

This shows the capability of a magnetic analyser to separate ions with different m/z ratios with respect to B or V . By scanning B or V it is then possible to focus, through the slit S_2 , all the ionic species generated inside the source, separated and ordered with respect to their m/z ratio. Dempster chose to perform the acceleration voltage scan, being difficult at that time to perform regular and reproducible B scans. Dempster called his instrument a ‘mass spectrometer’ but this definition was debated by Aston.¹⁶ In fact, using R from Equation (1.2) one can obtain:

$$R = mv/Bz \quad (1.4)$$

This relationship shows that all the ions entering the magnetic field and having the same charge and the same *momentum*, follow a circular pathway with an equal radius R , independently from their mass, while ions with different *momenta* follow pathways of different radii. For this reason, Aston suggested that the most appropriate term for Dempster’s instrument would be ‘momentum spectrometer’ and not ‘mass spectrometer’. However, for ions generated inside the ion source, Equation (1.3) is valid and the term ‘mass spectrometer’ is appropriate.

The physical application of mass spectrometers for the determination of natural isotope ratios and accurate mass of different nuclides gave rise to the development of instruments with high performance, in particular with increasing resolution. This led to the design of instruments based on the use of magnetic and electrostatic sectors.¹⁷ The researchers engaged in these developments determined that the resolution is mainly affected by four different factors:

- (i) ion beam spatial divergence;
- (ii) kinetic energy distribution of ions with the same m/z value;
- (iii) the curvature radius of the ion pathway inside the magnetic field;
- (iv) the width of the ion source and collector slit.

The ion beam emerging from an ion source is, in general, inhomogeneous either in direction or in kinetic energy. It means that the ion beam is partially divergent and consequently it enters in the analyser region with directions inside a θ angle. With respect to kinetic energy distribution, it must be taken into account that not all ions generated inside the ion source experiment the same accelerating field, the potential being inhomogeneous inside the source itself and, considering that $mv^2/2 = zV$, the V inhomogeneity is reflected in the kinetic energy inhomogeneity.

Both these negative aspects are corrected by the use of magnetic and electrostatic sectors.

In 1933 Stephens¹⁸ demonstrated that a magnetic sector leads to direction focusing of the ion beam. Just from the descriptive point of view let us consider the trajectory of an ion beam generated by the source *S* and focused by the magnetic field at the point *C* (Figure 1.12). The beam pathway is perpendicular to the field and follows the curve of radius *r*. If an ion enters the magnetic sector with an angle lower than 90°, it undergoes the field action for a longer time and consequently its deviation will be wider, leading to its focusing at *C*. If the angle is greater than 90° the residence time inside the magnetic field will be lower: its deviation will be smaller and the ion will again be focused at *C*. From the qualitative point of view, we can say that a magnetic sector focuses at the same point all ions having the same mass, charge and velocity. Hence, a magnetic sector exhibits not only a separating power, but also a focusing one. For these reasons, instruments employing a magnetic sector as a mass analyser were commonly called 'single focusing instruments', leading to direction focusing of the ion beam.

The use of electrostatic sectors is highly effective to overcome the inhomogeneity in kinetic energy. In these devices the ions are subjected to the action of a radial electrostatic field *E* with direction perpendicular to *B*. In the field *E*, generated by two parallel electrodes of cylindrical section (Figure 1.13), the ions are subjected to the action of a centripetal force zE . Calling mv^2/R their centrifugal force it will be:

$$zE = mv^2/R \quad (1.5)$$

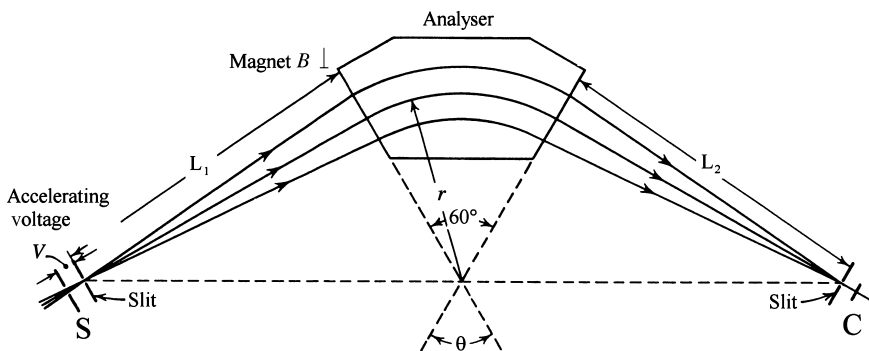


Figure 1.12 Direction focusing action of a magnetic sector

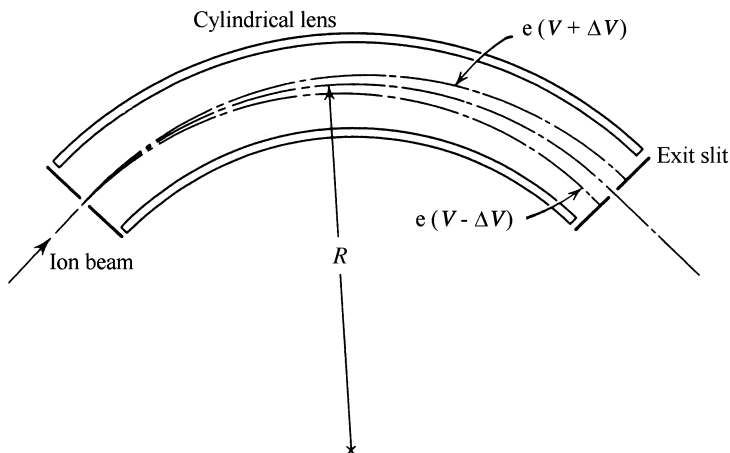


Figure 1.13 Velocity focusing action of an electrostatic sector

which, considering that $zV = \frac{1}{2}mv^2$, leads to the equation:

$$R = 2V/E \tag{1.6}$$

This equation shows that ions accelerated by V and subjected to the action of E follow a circular pathway of radius R , independently from their mass. For $E = \text{constant}$, only the ions with identical kinetic energy pass through the exit slit: the electrostatic sector consequently acts as a kinetic energy filter. Hence analysers employing B and E fields (for example, Figure 1.14) are called ‘double focusing instruments’.¹⁹

Double-focusing instruments exhibit a resolution up to 100 000. Of course the maximum value of resolution corresponds to very narrow slit width and consequently can be achieved in low sensitivity conditions.

1.2.3 Quadrupole Analysers

Quadrupole mass filter^{20,21} and quadrupole ion trap^{22,23} are currently the mass analysers most widely employed. They were both developed by the Paul group (Nobel Prize for physics in 1989) at Bonn University. The theoretical data of the behaviour of an ion in a quadrupole electrical field is highly complex. Here only a picture of such behaviour is given in order to give the reader a view of what is happening inside these devices.

Both systems start from the same considerations: ions of different m/z values will interact in a different manner with alternate electrical fields

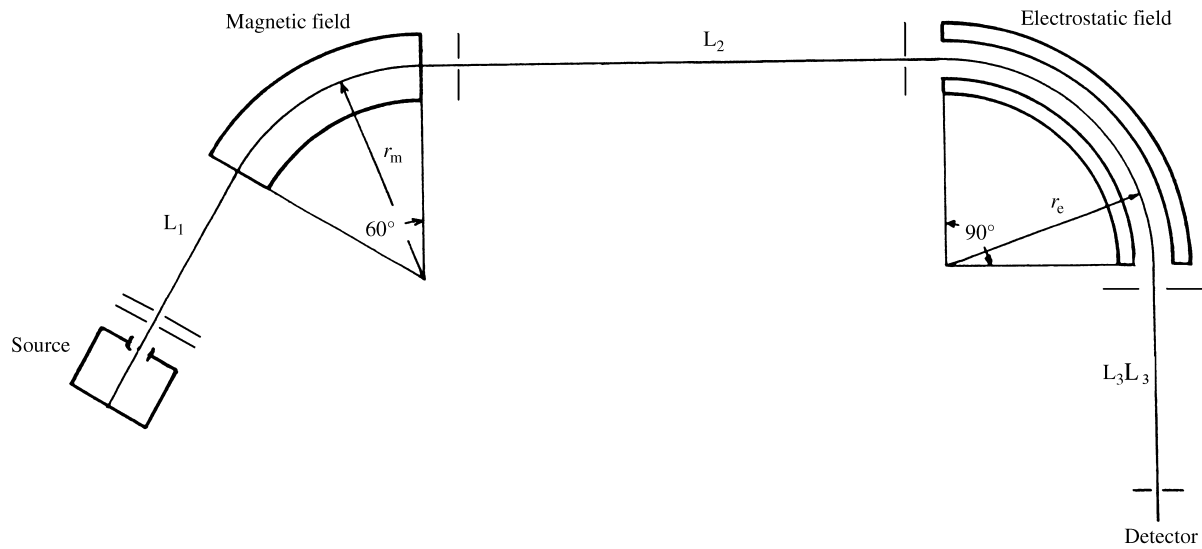


Figure 1.14 Scheme of a double focusing mass spectrometer. L_1 , first field-free region; L_2 , second field-free region

(radio frequency, RF). Many different devices were developed to study this interaction²¹ but, in the analytical world, the quadrupole mass filter and ion trap are the most widely employed.

1.2.3.1 *Quadrupole Mass Filter*^{20,21}

Let us consider an ion ejected from an ion source interacting with a quadrupole field generated by four hyperbolic section rods, as shown in Figure 1.15. On the rods a potential of the type $U \pm V \cos \omega t$ is applied (where U is the direct current potential and $V \cos \omega t$ is the RF potential). Ions which enter in this system oscillate in both x and y directions by the action of this field.

Let us consider the parameters that affect this motion; they are the ion m/z value, the U , V , ω values and r_0 , i.e. the dimension of the mass filter. If we define now two quantities taking into consideration all these parameters, i.e.:

$$a = 4zU/mr_0^2\omega^2 \quad (1.7)$$

$$q = 2zV/mr_0^2\omega^2 \quad (1.8)$$

it is possible to draw a 'stability diagram' of the device, i.e. to define the a and q values by which the ions follow 'stable' trajectories inside the

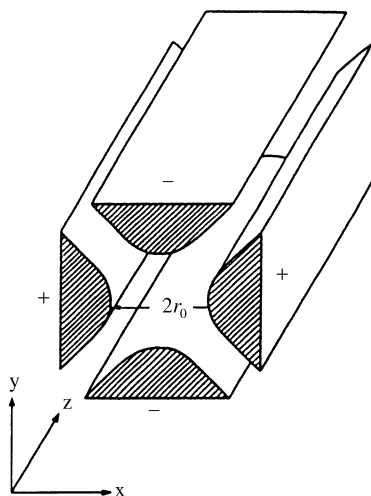


Figure 1.15 Quadrupole mass filter. The ions are injected in the z direction

inter-rod space. Outside this stability diagram the a and q values will be such that the ions will discharge on the rods. The stability diagram usually employed for a quadrupole mass filter is reported in Figure 1.16.

Looking at the a and q definitions it follows that ions with different m/z values exhibit different values of a and q . Furthermore, keeping U , V and ω constant, it is possible to overlap on the same diagram a straight line, whose slope is dependent on the a/q ratio. In fact, the a/q ratio can be calculated as:

$$a/q = (4zU/mr_0^2\omega^2)(mr_0^2\omega^2/2zV) = 2U/V \quad (1.9)$$

which leads to

$$a = (2U/V)q \quad (1.10)$$

This equation represents a straight line in the a, q space, crossing the origin of axes and whose slope is dependent on the U/V ratio. If we choose suitable values, a straight line as that reported in Figure 1.16 can be obtained. It just crosses the apex of the stability diagram and, in these conditions, all the ions exhibiting a and q values out from the apex will follow unstable trajectories. If the V and U values are increased, keeping the U/V ratio constant, ions will increase their a, q values (see Equations 1.7 and 1.8) and, when the straight line portion inside the apex of the stability diagram is reached, they will follow stable trajectories, passing through the rods and reaching the detector placed after the rods themselves. Hence, by scanning both U and V (maintaining the ratio $U/V = \text{constant}$) all the ions can be selectively detected.

The above described behaviour well explains the term ‘quadrupole mass filter’ of the device. One point to be emphasized is that by varying

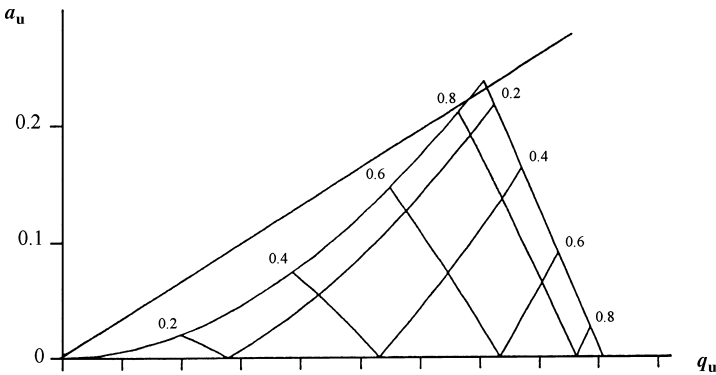


Figure 1.16 q, a stability diagram of a quadrupole mass filter

the U/V ratio it is possible to vary the straight line slope and consequently its portion inside the stability diagram. Using this approach it is possible to play on the peak width/ion current ratio. In other words, moving the straight line closer to the apex it is possible to obtain a better resolution but the sensitivity may show a significant decrease.

1.2.3.2 *Quadrupole Ion Trap*^{22,23}

The Paul ion trap is constituted by three electrodes arranged in a cylindrical symmetry (Figure 1.17). When a suitable $U + V\cos\omega t$ potential is applied on the intermediate electrode (ring electrode) and the two end-cap electrodes are grounded, a quadrupolar field is generated and the ions inside the trap follow trajectories confined in a well defined space region. Even in this case the behaviour of the ion trap can be described by defining a and q quantities analogous to those given for the quadrupole mass filter, leading to a stability diagram (Figure 1.18).

Most ion traps commercially available use, as potential applied to the ring electrode, only a RF voltage ($V\cos\omega t$). Consequently the stability

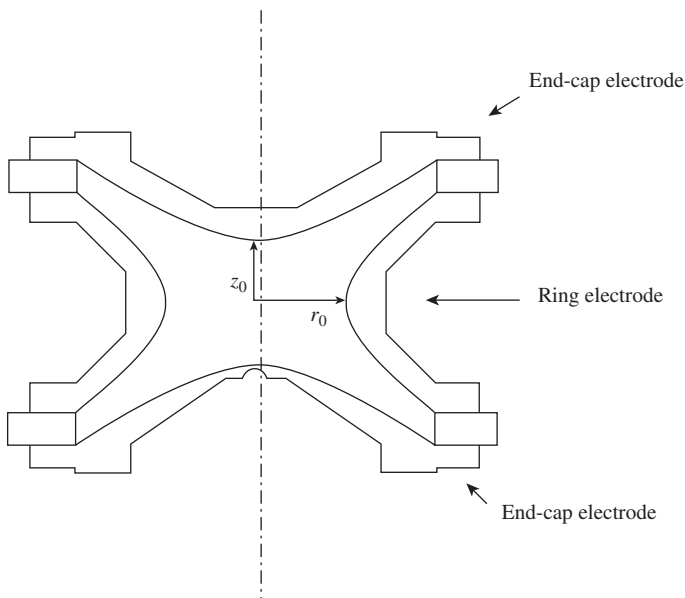


Figure 1.17 Quadrupole ion trap

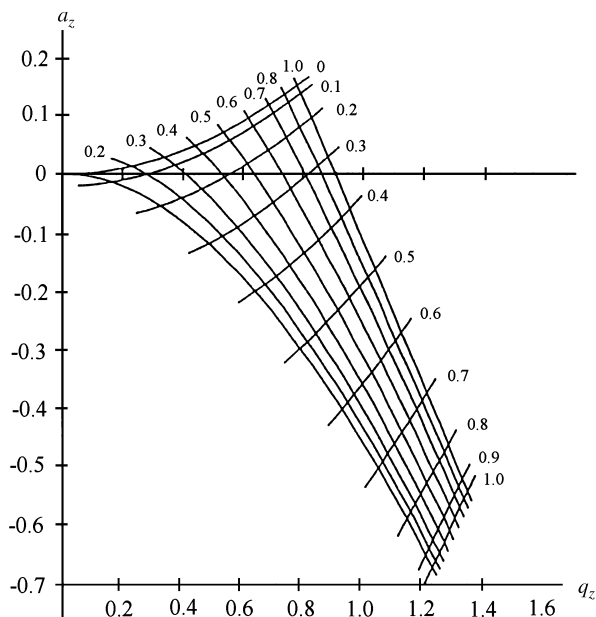


Figure 1.18 q, a stability diagram of a quadrupole ion trap

diagram related to the a, q pairs is in this case just a ‘stability line’ related to the q values only:

$$q = -4zV/mr_0^2\omega^2 \quad (1.11)$$

From this equation it follows that, for constant values of V, r_0 and ω , ions of different m/z values exhibit different q values and one can imagine different ions lying on the q axis at q values inversely proportional to their m/z values (Figure 1.19). If $m/z, V, r_0$ and ω values are appropriate, all the ions remain trapped inside the device. By scanning

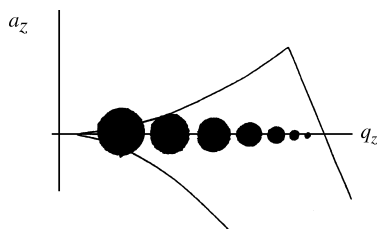


Figure 1.19 Portion of the stability diagram of a quadrupole ion trap. In the absence of U (DC) component, decreasing q values correspond to ions of increasing m/z values

V , the q values of the various ions increase and once their q value reaches the limit of the stability diagram their trajectory increases along the z axis: they are ejected from the trap and detected.

It is to be emphasized that the quadrupole ion trap has specific behaviour that makes it unique. First of all MS/MS experiments (which will be discussed in detail in Section 1.5.3) are easy to perform and the fragmentation yield is so high that sequential collisional experiments (MS^n) can be performed.²³ Secondly, the resolution available by ion trap has been proven to be up to 10^6 .²³ Unfortunately, instruments with these latter performances are not still available and only resolution of a few thousand are present in commercial instruments, employed only for partial portions of the mass spectrum. Furthermore two other points are worth noting: on the one hand, the theoretical high mass range available, obtained by the use of a supplementary RF voltage (ion trap with mass range up to m/z 8000 are available); on the other, the high sensitivity of the device (ions produced are not lost during the scanning).²³ These facilities have led to the production of an ion trap with powerful performances for gas chromatography/mass spectrometry (GC/MS) and LC/ESI(APCI)/MS systems.

1.2.4 Time-of-flight

Time-of-flight (TOF)²⁴ is surely, from the theoretical point of view, the simplest mass analyser. In its 'linear' configuration it consists only of an ion source and a detector, between which a region under vacuum, without any field, is present. Ions with a m/z accelerated by the action of a field V acquire a speed v . The potential energy will be equal to the acquired kinetic energy (Equation 1.1). If, from this equation, we put in the v value:

$$v = [(2zV/m)]^{1/2} \quad (1.12)$$

it is easy to observe that ions of different m/z values exhibit different speeds, inversely proportional to the square root of their m/z values. If the ion follows a linear pathway inside a field-free region of length l , considering that $v = l/t$, i.e. $t = l/v$, it follows that:

$$t = l(m/2zV)^{1/2} \quad (1.13)$$

This equation shows that ions of different m/z value reach the detector at different times, proportional to the square root of their m/z value. For this reason this device is called 'time-of-flight' (Figure 1.20).

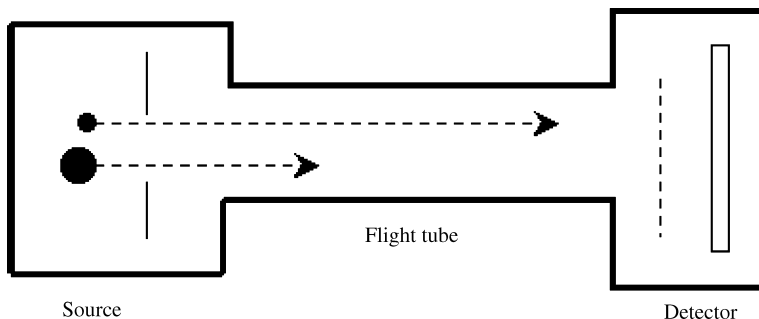


Figure 1.20 Scheme of a linear TOF mass analyser

The calibration of the time scale with respect to m/z value can be easily obtained by injection of samples of known mass.

Of course, this analyser cannot operate in a continuous mode as the sector and quadrupole ones. In this case, an ion pulsing phase is required: the shorter the pulse, the better defined is the mass value and the peak shape.

Furthermore, the ions emerging from the source are usually not homogenous with respect to their speed (this effect mainly arises from the inhomogeneity of the acceleration field). Of course, a distribution of kinetic energy will reflect immediately on the peak shape and wide kinetic energy distribution will lead to enlarged peak shape, with the consequent decrease in resolution. To overcome this, different approaches have been proposed and that usually employed consists of a reflectron device. As shown in Figure 1.21, the reflectron is constituted by a series of ring electrodes and a final plate. The plate is placed at a few hundred volts over the V values employed for ion acceleration. By using a series of resistors, the different ring electrodes are placed at decreasing potentials. When an ion beam with kinetic energy $E_k \pm \Delta E_k$ interacts with this field, the ion with excess kinetic energy ($E_k + \Delta E_k$)

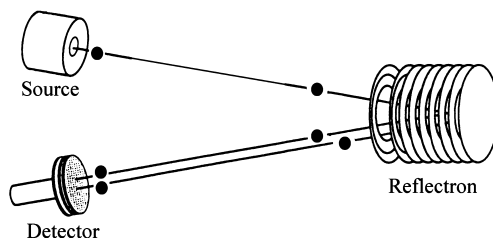


Figure 1.21 Scheme of reflectron TOF

will penetrate that field following a pathway longer than that followed by ions with mean kinetic energy E_k . In contrast, ions with lower kinetic energy will follow a shorter pathway. This phenomenon leads to a thickening of the ion arrival time distribution with a consequent, significant increase in mass resolution.

Nowadays, TOF systems with resolution up to 20 000 are commercially available.

1.3 GC/MS²⁵

The coupling of a mass spectrometer with a gas chromatographic system was realized in the 1960s and immediately the scientific community recognized the high power of the system. In the beginning the only chromatographic columns available were packed ones, operating with carrier gas flows in the order of 10 mL/min. Considering the simple relationship between pumping speed (P , L/s) and gas flow (f , mL/min) corresponding to the maintenance of a vacuum in the order of 10^{-5} Torr:

$$P = 10^3 f \quad (1.14)$$

It follows that a direct coupling of a packed column with a mass spectrometer is practically impossible and consequently the use of a He separator was necessary. This led, at the beginning of GC/MS development, to severe limitations of the system, which completely disappeared when capillary columns were introduced. Nowadays, GC/MS systems are robust, reliable, sensitive and highly specific instruments. Their main power is due to the fact that they can be effectively employed for qualitative and quantitative analyses. In most systems, the chromatographic column directly reaches the ion source, usually operating in EI and CI conditions.

The system can operate in three different modes, briefly described below.

1.3.1 Total Ion Current (TIC) Chromatogram

The chromatogram is obtained by sequential MS scanning (typical times are in the order 0.2–0.5 s); the data system takes the sum of the signal due to different ions present in each spectrum (TIC) and plots the signal so

obtained with respect to the analysis time. The chromatograms are consequently related to the TIC due to the background (baseline) and to the different components eluting from the chromatographic column (chromatographic peaks).

For quantitative analysis it must be taken into consideration that different compounds exhibit a different ionization yield and consequently lead to a different TIC signal. For such a reason, the use of an internal standard (IS) is essential to obtain reliable quantitative data. These aspects will be discussed in detail in Chapters 2 and 3.

For the qualitative point of view, once the data file corresponding to the TIC chromatogram is obtained, it is easy to obtain the mass spectra of various components by just looking at the data with respect to their retention time.

1.3.2 Reconstructed Ion Chromatogram (RIC)

The data file obtained by the TIC approach can be validly employed to confirm the presence of and to quantify species of interest present in a complex mixture. Using the data it is possible to select one or more ions of interest and reconstruct a chromatogram related to their m/z value only. By this approach a high specificity can be achieved and practically an increase of chromatographic resolution can be obtained.

For example, in Figure 1.22 the TIC chromatogram shows a wide peak in the range 12.5–17 min, but when the ion chromatograms

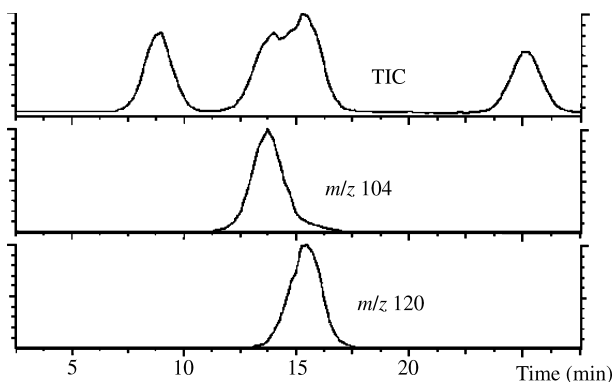


Figure 1.22 Gas chromatograms obtained by TIC and ion current related to ions at m/z 104 and 120

relating to m/z 104 and 120 values are reconstructed, it is found that the peak is due to the partial overlapping of two different components.

1.3.3 Multiple Ion Detection (MID)

In the case of trace analysis, it is useful not to perform the scan of all the spectra, but to consider the different m/z values characteristic of the mass spectrum of the compound of interest. Using this approach, a higher speed monitoring of the chromatographic eluate can be obtained and valid quantitative data are obtained even for species present at ppb level. This approach can be applied either on mass units or on accurate mass values, leading to an increase of specificity of the method.

1.4 LC/MS²⁶

In the beginning, the coupling of LC with traditional (EI, CI) sources was unsuccessful, due to the high solvent level present in LC eluate. Some attempts were made to remove the solvent by 'moving belt' systems and to use the solvent itself as reactant for low pressure CI experiments. The situation changed with the development of atmospheric pressure ion sources, such as in APCI, ESI and, to a minor extent, APPI.

Nowadays these systems are widely employed and allow the application of mass spectrometry in fields (especially biological and biomedical) which only a few decades were completely off limits.

A typical arrangement for LC/MS measurements is shown in Figure 1.23. It consists of a LC pump, LC column, APCI or ESI source and mass spectrometer. The LC pump system and the LC column must be chosen considering the source employed. In fact, due to the different ionization mechanisms, each source has its own optimum eluent flow rate and solvent polarity. The APCI source operates properly with eluent flow rates higher than those employed for ESI and is compatible with a

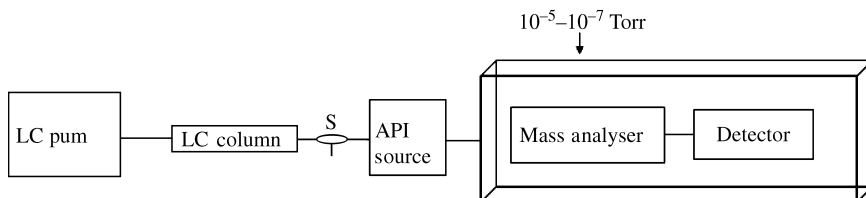


Figure 1.23 Scheme of the LC/MS coupling

nonpolar mobile phase. Typical eluent flow rates employed with an APCI source are in the range 4.0–0.5 mL/min: below 0.4 mL/min an unstable analyte signal can be observed due to nonreproducible discharge processes. This implies the use of a conventional LC pump and normal (3–4.6 mm ID) and narrow-bore (1–2 mm ID) LC column.

A modern ESI source can work with eluent flow rate up to 1 mL/min, even if the optimum value is about 0.2–0.3 mL/min. A normal LC column can be used by splitting the eluent before the entrance in the ESI source, while narrow-bore LC columns are normally employed without splitting. The most recent ESI developments lead to micro-ESI and nano-ESI, employed for high sensitivity measurements and applications where sample amounts are limited (i.e. proteomic, pharmacokinetic studies, etc.). Flow rates in the range 100–10 000 nL/min are normally used and can be obtained by a capillary LC pump, equipped with a capillary (0.15–0.8 mm ID) and nano (20–100 μm ID) LC column.

As in the case of GC/MS, TIC chromatogram, RIC and MID can be obtained.

1.5 MS/MS²⁷

MS/MS is based on the use of a first mass analyser, employed to select ions of interest, and a second mass analyser devoted to the analysis of the decomposition products of the preselected ions.

The MS/MS experiment can be subdivided into four different steps:

- (i) ion generation;
- (ii) ion selection;
- (iii) selected ion decomposition;
- (iv) mass analysis of the selected ion decomposition products.

These steps can occur in different space regions and in this case the experiment is called MS/MS ‘in space’, or in the same space region and consequently they must be time separated. The latter approach is called MS/MS ‘in time’.

1.5.1 MS/MS by Double Focusing Instruments

The first experiments of MS/MS were generated by the study of the naturally occurring decomposition of selected ions in the region between

the magnetic and electrostatic sector of a double focusing instrument (see, for example, Figure 1.14).²⁸ The ions of interest, produced in the ion source, were selected by fixing the related B value. The decomposition products were analysed by scanning the electrostatic sector. In order to increase the yield of ion fragmentation a ‘collision cell’, i.e. a small box in which a collision gas (typical pressures in the range 10^{-2} – 10^{-3} Torr) was inserted in that region, and a fantastic increase of product ion abundance number and abundance was observed. The method was called collisional-induced decomposition (CID) and in the first years of its application its main use was in the field of structural analysis of gaseous ions.

However, in the 1980s some papers appeared, showing the power of the method in the analysis of compounds of interest present in complex mixtures. In fact, without the use of any separative method, it is possible, by direct introduction of a complex mixture and selection of the ion characterizing the analyte, to determine its presence and, in some cases, to obtain some quantitative data.

1.5.2 MS/MS by Triple Quadrupoles

The real introduction of the MS/MS system in the analytical world started with the development of triple quadrupole (QQQ) systems,²⁹ shown schematically in Figure 1.24. The ions of interest (M^+), produced by the suitable ionization method, are selected by Q_1 , by choosing the appropriate U and V values. The collision gas is injected in Q_2 , which operates in RF only (i.e. it behaves as an ion lens). The ions originating by collisionally induced decomposition of M^+ are analysed by Q_3 .

This instrumental arrangement allows a wide series of collisional experiments to be performed, among which the most analytically relevant are:

- (i) product ion scan: identification of the decomposition product of a selected ionic species;

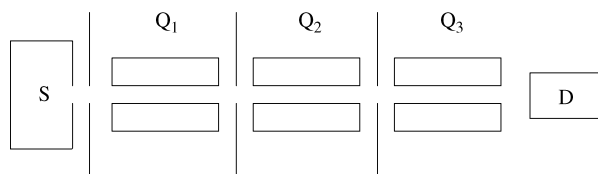


Figure 1.24 Scheme of a triple quadrupole (QQQ) system for MS/MS experiments

- (ii) parent ion scan: identification of all the ionic species which produce the same fragment ion;
- (iii) neutral loss scan: identification of all the ionic species which decompose through the loss of the same neutral fragment.

The collisional phenomena occurring in a triple quadrupole (as well as in sector machines) lead to the production of an ion population with a wide internal energy distribution, due to the statistics of the preselected ion – target gas interactions. Hence, various decomposition channels, exhibiting different critical energies, can be activated and the resulting MS/MS spectrum is, in general, particularly rich of peaks and, consequently, of analytical information.

What are the parameters which one can vary in a MS/MS experiment by QQQ? Two parameters are the nature of the target gas (the larger the target dimension, the higher the internal energy deposition on the preselected ion: in other words, Ar is more effective than He) and its pressure (the higher the pressure, the higher the probability of multiple collisions leading to increased decompositions: of course the pressure must not exceed the limit compromising the ion transmission!). But, over all, the kinetic energy of colliding ions, which can be varied by suitable electrostatic lenses placed between Q_1 and Q_2 , plays a fundamental role in MS/MS experiments.

1.5.3 MS/MS by Ion Traps

More recently, ion trap showed interesting behaviour for MS/MS experiments.²³ It represents an example of MS/MS ‘in time’. In fact, the sequence ion isolation – collision – product ions analysis is performed in the same physical space and consequently must be time-separated. A typical sequence is reported in Figure 1.25.

The ions are generated inside the ion trap (or injected in the trap after their outside generation) for a suitable time, chosen in order to optimize the number of trapped ions (a too high ion density leads to degraded data due to space-charge effects). The ions inside the trap exhibit motion frequency depending on their m/z values. The ion selection phase is achieved by the application, on the two end-caps, of a supplementary RF voltage with all the ion frequencies but the ion of interest one. In these conditions all the undesired ions are ejected from the trap and only that of interest remains trapped. The collision of the preselected ion is again performed by resonance with the supplementary RF field with a frequency

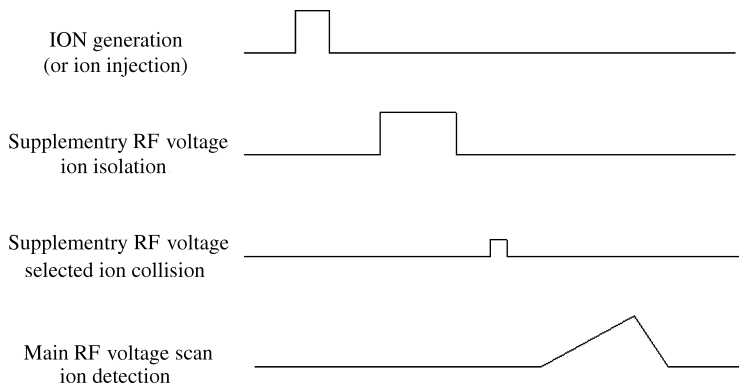


Figure 1.25 Sequential pulses of supplementary and main RF voltages employed to perform MS/MS experiments by ion trap

corresponding to that of ion motion, but with an intensity such to maintain the ion trajectory inside the trap walls. The ion collides with the He atoms, present in the trap as buffer gas and, once sufficient internal energy is acquired, it decomposes: the product ions so generated remain trapped and by the main RF scan they are ejected from the trap and detected.

It should be emphasized that the collisional data obtained by ion trap are quite different from those achieved by QQQ. In fact in this case the energy deposition is a step-by-step phenomenon.³⁰ Each time that the ion is accelerated by the supplementary RF field up and down inside the trap, it acquires, through collision with He atoms, a small amount of internal energy. When the internal energy necessary to activate the decomposition channel(s) at the lowest critical energy is reached, the ion fragments. In other words, while in the case of QQQ the wide internal energy distribution from collisional experiments leads to the production of a large set of product ions, in the case of ion trap only a few product ions are detected, originating from the decomposition processes at lowest critical energy.

This aspect could be considered negative from the analytical point of view: in fact a better structural characterization can be achieved by the presence of a wider product ions set. But it can be easily and effectively overcome by the ability of ion trap to perform multiple MS/MS experiments. In fact the sequence shown in Figure 1.25 can be repeated by selection, among the collisionally generated product ions, of an ionic species of interest, its collision and the detection of its product ions (MS³). This process can be repeated more times (MSⁿ), allowing on the one hand to draw a detailed decomposition pattern related to low energy

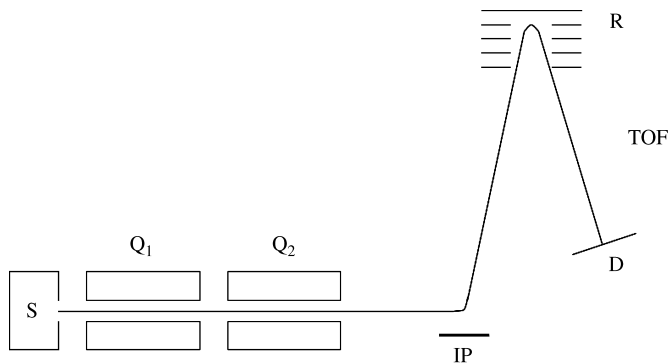


Figure 1.26 Scheme of a Q-TOF system. S, ion source; Q₁, quadrupole for the selection of ionic species of interest; Q₂, collision region (Q₂ operates in RF only); IP, ion pusher; R, reflectron; D, detector

decomposition channels, and on the other to obtain fragment ions of high diagnostic value from the structural point of view (and hence analytically highly relevant). Hence, by ion trap it is possible to perform MSⁿ experiments, which cannot be obtained by the QQQ approach.

1.5.4 MS/MS by Q-TOF

Recently a new MS/MS instrument has become available, exhibiting a specificity higher than that achieved by QQQ or ion trap systems. It is based on a 'hybrid' configuration, employing mass analysers based on different separation principles. The system, usually called Q-TOF is shown schematically in Figure 1.26. The ion of interest, generated in the source S, is selected by the quadrupole mass filter Q₁. Collisions take place in Q₂ (a quadrupole operating in RF only). The product ions are analysed by a TOF analyser. Considering the high resolution conditions available by TOF, by this approach the accurate masses of the collisionally generated product ions (as well as of the precursor) can be easily obtained, allowing the determination of their elemental composition. This possibility leads to a significant increase in the specificity of MS/MS data.

REFERENCES

1. T. D. Mark and G. H. Dunn (Eds) *Electron Impact Ionization*, Springer-Verlag, Wien (1985).

2. A. G. Harrison, *Chemical Ionization Mass Spectrometry*, CRC Press, Boca Raton (1983).
3. S. G. Lias, J. E. Bartness, J. F. Liebmann, J. L. Holmes, R. D. Levin and W. G. Mallard, *J. Phys. Chem. Ref. Data*, **17** (Suppl. 1) (1988).
4. H. D. Beckey, *Principles of Field Ionization and Field Desorption Mass Spectrometry*, Pergamon, London (1975).
5. M. Barber, R. S. Bordoli, G. J. Elliott, R. D. Sedgwick and A. N. Tyler, *Anal. Chem.*, **54**, 645–657A (1982).
6. A. P. Bruins, *Mass Spectrom. Rev.*, **10**, 53–77 (1991).
7. (a) M. Yamashita and J. B. Fenn, *J. Phys. Chem.*, **88**, 4451–4459 (1988); (b) M. Yamashita and J. B. Fenn, *J. Phys. Chem.*, **88**, 4671–4675 (1988).
8. D. B. Robb, T. R. Covey and A. P. Bruins, *Anal. Chem.*, **72**, 3653–3659 (2000).
9. M. Karas, D. Bahar and U. Griessmann, *Mass Spectrom. Rev.*, **10**, 335–357 (1991).
10. R. J. Pfeiffer and C. D. Hendricks, *AIChE J.*, **6**, 496–502 (1968).
11. G. L. Taylor, *Proc. R. Soc. London Ser. A*, **280**, 383–387 (1964).
12. M. Dole, L. L. Mack, R. L. Hines, R. C. Mobley, L. D. Ferguson and M. B. Alice, *J. Chem. Phys.*, **49**, 2240–2249 (1968).
13. J. V. Iribarne and B. A. Thomson, *J. Chem. Phys.*, 2287–2294 (1976).
14. P. Traldi and E. Marotta in *Advances in Mass Spectrometry*, Vol. 16, A. E. Ashcroft, G. Brenton and J. J. Monagan (Eds), Elsevier, Amsterdam (2004), pp. 275–293.
15. A. J. Dempster, *J. Phys. Rev.*, **11**, 316–320 (1918).
16. F. W. Aston, *Nature*, **127**, 813–820 (1931).
17. (a) J. H. Beynon in *Mass Spectrometry and its Applications to Organic Chemistry*, Elsevier, Amsterdam (1960), pp. 4–27; (b) F. A. White and G. Wood in *Mass Spectrometry Applications in Science and Engineering*, John Wiley & Sons, Inc., New York (1986), pp. 51–66.
18. W. E. Stephens, *Phys. Rev.*, **45**, 513–518 (1934).
19. (a) F. A. White, F. M. Rourke and J. M. Sheffield, *Appl. Spectr.*, **12**, 46–52 (1958); (b) T. Wachs, P. F. Bente and F. W. McLafferty, *Int. J. Mass Spectrom. Ion Phys.*, **9**, 333–341 (1972); (c) J. H. Beynon, R. G. Cooks and J. W. Amy, *Anal. Chem.*, **45**, 1023 (1973); (d) H. Hintenberger and L. A. König, *Z. Naturforsch. A*, **12**, 443–452 (1957); (e) R. P. Morgan, J. H. Beynon, R. H. Bateman and B. N. Green, *Int. J. Mass Spectrom. Ion Phys.*, **28**, 171–191 (1978).
20. (a) W. Paul and H. Steinwedel, Ger. Pat. 944, 900 (1956); US Pat. 2, 939, 952 (1960); (b) W. Paul and H. Steinwedel, *Z. Naturforsch. A*, **8**, 44 (1953); (c) W. Paul, H. P. Reinhard and U. von Zahn, *Z. Phys.*, **152**, 153 (1958).
21. P. H. Dawson (Ed.) *Quadrupole Mass Spectrometry and its Applications*, Elsevier, Amsterdam (1976).
22. R. E. March and R. J. Hughes, *Quadrupole Storage Mass Spectrometry*, John Wiley & Sons, Inc., New York (1989).
23. R. E. March and J. F. J. Todd (Eds) *Practical Aspects of Ion Trap Mass Spectrometry*, Vols I–III, CRC Press, Boca Raton (1995).
24. (a) W. C. Wiley and I. H. McLaren, *Rev. Sci. Instr.*, **26**, 1150–1157 (1955); (b) R. J. Cotter, *Anal. Chem.*, **64**, 1027A–1039A (1992); (c) B. A. Mamyurin, V. I. Karataev, D. V. Shmikk and V. A. Zagulin, *Sov. Phys.-JETP*, **37**, 45–48 (1973); (d) B. A. Mamyurin, *Int. J. Mass Spectrom. Ion Proc.*, **131**, 1–19 (1994).
25. J. Abian and E. Gelpi in *Mass Spectrometry in Biomolecular Sciences*, R. Caprioli, A. Malorni and G. Sindona (Eds), NATO ASI Series, Series C: Mathematical and

- Physical Sciences, Vol. 475, Kluwer Academic Publisher, Dordrecht (1996), pp. 437–460.
26. (a) B. E. Erickson, *Anal. Chem.*, **72**, 711A–716A (2000); (b) W. M. Niessen, *J. Chromatogr. A*, **856**, 179–197 (1999).
 27. F. W. McLaffery (Ed.) *Tandem Mass Spectrometry*, John Wiley & Sons, Inc., New York, (1983).
 28. R. G. Cooks, J. H. Beynon, R. M. Caprioli and G. R. Lester, *Metastable Ions*, Elsevier, Amsterdam (1973).
 29. R. A. Yost and C. G. Enke in *Tandem Mass Spectrometry*, F. W. McLaffery (Ed.), John Wiley & Sons, Inc., New York (1983), pp. 175–195.
 30. J. Gronova, C. Paradisi, P. Traldi and U. Vettori, *Rapid Commun. Mass Spectrom.*, **4**, 306–313 (1990).